

GAS-DYNAMIC SPRAYING.

STUDY OF A PLANE SUPERSONIC TWO-PHASE JET

A. P. Alkhimov, S. V. Klinkov,
V. F. Kosarev, and A. N. Papyrin

UDC 621.793+533.6.011

The rigorous demands of practice necessitate the creation and development of advanced resource-saving scientific technologies. These technologies include, in particular, deposition of powder coatings (protective, reinforcing, current-conducting, etc.). Among the presently known spraying techniques, gas-thermal (gas-flame, plasma, detonation, etc.) ones that allow one to form coatings of various materials and to ensure a wide range of physical and chemical parameters and utilization properties are the most promising. The merits and demerits of these techniques are widely known [1-3]. The area of their applicability is mainly limited by the use of high-temperature jets ($2 \cdot 10^3$ – $5 \cdot 10^4$ K).

Thus, the previously found effect of formation of coatings of solid-state aluminum particles on the frontal surface of bodies exposed to a supersonic two-phase flow with stagnation temperature $T_0 \sim 300$ K is of great scientific and practical importance. The deposition method based on this effect was called the method of "cold" gas-dynamic spraying [4]. The wide practical application of this technique required its realization in a two-phase jet-moving target regime, which called forth the necessity of studying a plane supersonic two-phase jet, in particular, the character of a jet flowing into an obstacle, and measuring the velocities of particles with diameters of $d_p \leq 50 \cdot 10^{-6}$ m in this jet, etc. The results of such studies are presented in this paper.

1. Experimental Setup and Methods of Diagnostics. For an effective particle acceleration in the supersonic section of a nozzle, it is necessary that its length be not less than the relaxation length of the particles used for deposition. For typical values of the relative particle velocity $\Delta v = v - v_p \sim 100$ m/sec particle density $\rho_p \simeq 5 \cdot 10^3$ kg/m³, gas density $\rho \simeq 3$ kg/m³ and viscosity $\mu \simeq 10^{-5}$ kg/(m·sec), and for Reynolds number $Re = \Delta v d_p \rho / \mu \approx 10^3$, estimation of the relaxation length l_r of the particles with diameter $d_p = 50 \cdot 10^{-6}$ m accelerated in a supersonic nozzle with the Mach number $M = 2.0$ – 3.0 yields $l_r = 4(e - 2)\rho_p d_p / 3\rho \simeq 0.1$ m (in an estimation, for such Re the particle drag coefficient C_x was assumed to be equal to unity). In approaching the substrate, the particle is decelerated in the compressed layer formed by the supersonic jet flowing to the target. The estimates show that the particle velocity ($d_p \simeq 5 \cdot 10^{-6}$ m and $\rho_p \simeq 5 \cdot 10^3$ kg/m³) decreases in the compressed layer by a factor of e over of $\sim 3 \cdot 10^{-3}$ m. In view of this effect and also the fact that the compressed-layer thickness is mainly determined by a smaller transverse size of the jet, we used nozzles with a throat determined by the height b^* and by the thickness of the contoured inserts $h = (1-5) \cdot 10^{-3}$ m. The exit cross section of the Laval nozzle $H \times h$ corresponded to $M = 2.0$ – 3.0 without account of the displacing effect of the boundary layer.

To study experimentally various parameters of the plane supersonic jet exhausted from such nozzles, a special facility was designed and fabricated. Figure 1 shows its layout and methods of diagnostics. The main members of this facility are a supersonic plane nozzle 1, a particle dosimeter 2, and a gas heater 3 with a heating-temperature control system 4. As working gases, we utilized the air 5 and also the compressed gas — helium or argon from a gas holder 6. The pressure in the plenum chamber, at the nozzle exit, and in the dosimeter was controlled by manometers 7–9. The feeding system of the facility allowed one to obtain gas mixtures of a definite composition, and, as a result, the exhaust velocity of the gas at the nozzle exit

Institute of Theoretical and Applied Mechanics, Siberian Division, Russian Academy of Sciences. Novosibirsk 630090. Translated from *Prikladnaya Mekhanika i Tekhnicheskaya Fizika*, Vol. 38, No. 2, pp. 176–183, March–April, 1997. Original article submitted November 29, 1995.

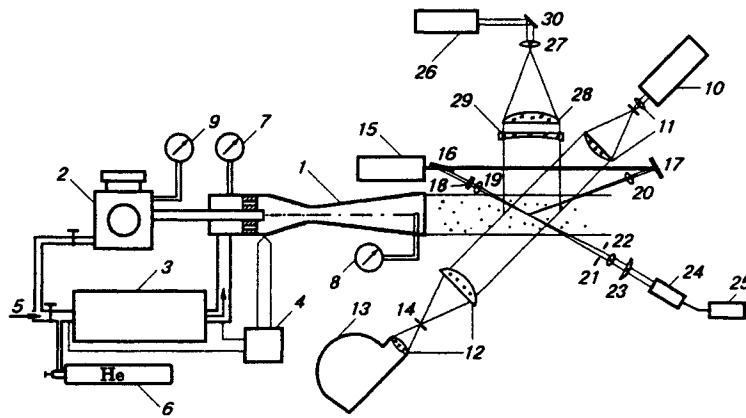


Fig. 1

could be varied over wide limits from the pure-air velocity (560 m/sec for $M=2.6$) to the pure-helium velocity (1400 m/sec for $M=2.6$) in the design exhaust regime. As further investigations have shown, the particle velocity could also be varied over very wide limits. The methods of diagnostics included:

- methods of fast-response laser visualization;
- registration of particle trajectories by the laser-“knife” method;
- measurements with a laser-Doppler anemometer (LDA) with direct spectral analysis;
- measurement of the particle velocity in the jet by the tracking method.

The facility also allowed us to measure the gas-velocity distribution over the jet using a total-pressure probe.

2. Jet Visualization. The free gas jet and the jet that flows into an obstacle have been studied theoretically and experimentally (see, e.g., [5]). However, the conditions of our experiments lead to the appearance of some characteristics which are attributed to the unusual geometry of the nozzles: the large aspect ratio and the rectangular exit cross section with a small value at one of the sides when the boundary layer at the nozzle walls can play an essential role. In view of this, it would be desirable to visualize the flow structure to choose an optimum nozzle-operation regime and the best position of the substrate relative to its exit cross section, and also to determine the position of the central shock wave ahead of the target, which is important for evaluation of the effect of particle deceleration in the compressed layer. Jet photoregistration was performed by the method of fast-response laser visualization whose scheme is presented in Fig. 1. The light source was a ruby laser 10 operating in a modulated Q-factor regime with pulse duration $\tau = 30 \cdot 10^{-9}$ sec. The light beam was formed by a telescopic system 11, and the image of the object to be study was formed by detecting optics 12 and was registered by a camera 13. A visualizing element 14 was placed in the focus of detecting optics. This element was either a metal ball acting as a symmetric knife or a visualizing diaphragm.

We examined helium and air jets with nozzle pressure ratio $n = 0.6-2.5$ which were exhausted from the nozzles with the accelerating-section length $L = 0.07, 0.1, \text{ and } 0.13$ m and $M = 2.35, 2.12, \text{ and } 2.01$, respectively.

Figure 2 shows typical instantaneous ($\tau = 30 \cdot 10^{-9}$ sec) photographs of the air jet with $M=2.01$ exhausted into the ambient medium for various nozzle-pressure ratios [(a)–(c) correspond to $n = 1, 1.5, \text{ and } 2$] and also the photograph of the helium jet exhausted in the design regime (d). Analysis of numerous photographs shows that the air jet exhausted in the design regime remains intact up to a distance of 6–10 jet diameters from the nozzle exit. It follows from the data obtained that the gas velocity and, hence, the particle velocity in the core of the design air jet change insignificantly at distances equal to 0–10 jet diameters from the nozzle exit.

As was mentioned earlier, the rate of the particle–substrate interaction is determined not only by the velocity the particle being accelerated in a supersonic nozzle acquires, but also by how much it is decelerated in the compressed layer between the shock wave and the substrate surface. Therefore, our special interest was

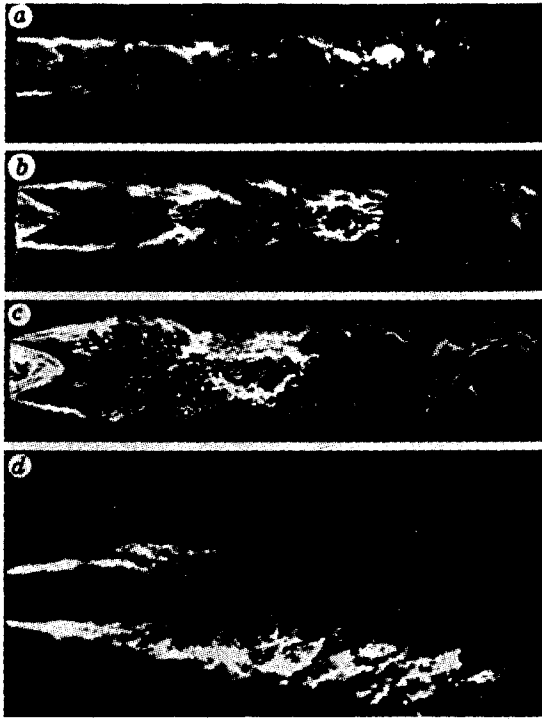


Fig. 2

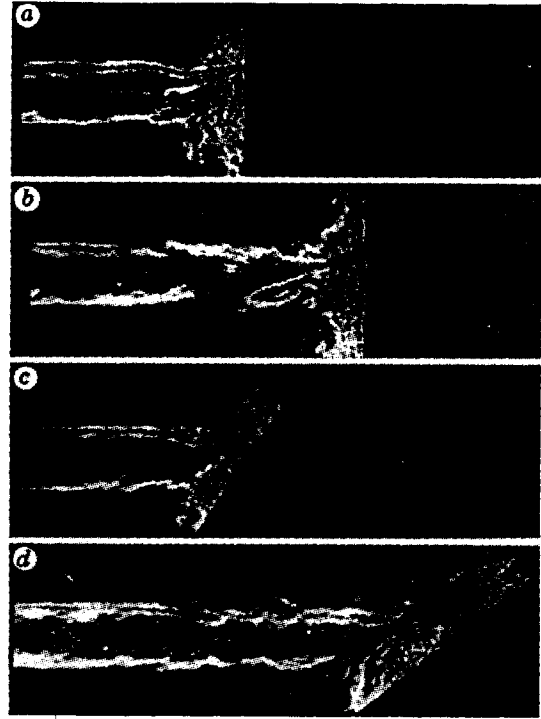


Fig. 3

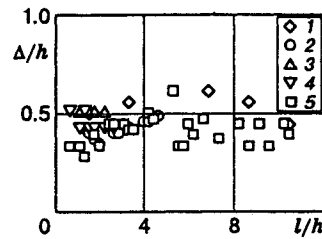


Fig. 4

to study a plane supersonic jet flowing into a target.

Figure 3a and b shows typical schlieren pictures of the design air jet with $M = 2.35$ flowing perpendicularly into the target. The distance between the nozzle exit and the target was varied within the range of 0–10 jet diameters. The compressed-layer thickness measured from the photographs showed that it depends weakly on the distance from the nozzle exit to the target, the latter being varied from 0 to ~ 10 diameters of the jet. This is clearly seen from Fig. 4 in which the distance from the nozzle exit to the target which was normalized to a smaller size of the exit cross-section h of the nozzle is plotted as the abscissa, and the ratio of the compressed-layer thickness to h which was varied from $1 \cdot 10^{-3}$ (points 3) to $2.3 \cdot 10^{-3}$ (points 4), $3 \cdot 10^{-3}$ (points 1 and 5), and $5 \cdot 10^{-3}$ m (points 2) is plotted as the ordinate. One can see that Δ/h varies within the range of 0.3–0.6 for different nozzles, with a mean value of ~ 0.4 .

Obviously, in approaching the nozzle and target closer than $l_{\min} = 0.4h$, the central shock will enter the nozzle, and the flow regime will be violated. Therefore, l_{\min} can be regarded as a minimum distance for powder deposition. Studying the character of interaction of the design air jet with the target at angles of 60° , 45° , and 30° for various distances from the nozzle exit to the target showed that the character of this

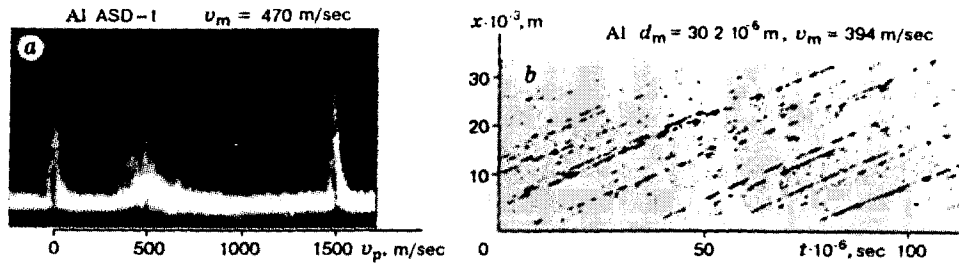


Fig. 5

interaction at different angles is also weakly dependent on the distance between the nozzle exit and the target. Figure 3 shows typical photographs of the jet at angles of 60 and 45° [(c) and (d)]. Note that the flow pattern and, in particular, the position of the central shock changed weakly when the jet contained aluminum particles even at sufficiently high disperse-phase flow rates [$Q_1 = 40 \text{ kg}/(\text{sec} \cdot \text{m}^2)$], which corresponds to the volume concentration $\varphi \simeq 10^{-4}$. This allowed us to use the results for a pure jet in further investigations of a two-phase jet with a moderate disperse-phase concentration ($\varphi \leq 10^{-4}$).

3. Estimates of the Boundary-Layer Thickness. As has been already noted, when nozzles with unusual geometric characteristics are used (a large aspect ratio and a rectangular exit cross section with a small value at one of the sides), the boundary layer formed at the side walls of the supersonic section of the nozzle can play an essential part.

Let us estimate the boundary-layer displacement thickness at the nozzle-exit cross section for $M = 3$, $T_0 = 300 \text{ K}$, and static pressure $p = 0.1 \text{ MPa}$ assuming that the boundary layer is formed on a flat plate in a gradientless flow and is fully turbulent. For the above gas-flow parameters, typical length of the accelerating section of the nozzle $L = 0.1 \text{ m}$, and static temperature $T_{st} = T_0/(1+0.2M^2) = 110 \text{ K}$, we obtain $Re = 2.5 \cdot 10^7$. The momentum-loss thickness on the flat plate in gradientless flow is $\delta^{**} = LC_F/2$. Here $C_F = \Psi_M C_{F0}$, where C_{F0} is the mean friction coefficient in an incompressible flow (from the data of [6], $C_{F0} = 0.0027$), and Ψ_M accounts for the compressibility (according to [7], $\Psi_M = 0.6$). Hence, under the above conditions, on the flat plate we have $\delta^{**}/L = 0.00081$, and, for $L = 0.1 \text{ m}$, we have $\delta^{**} = 81 \cdot 10^{-6} \text{ m}$. For $M = 3$, the form parameter is $H = \delta^*/\delta^{**} = 5$ [7] in the absence of heat transfer, which yields the displacement thickness $\delta^* = 0.4 \cdot 10^{-3} \text{ m}$ that characterizes the displacing effect of the boundary layer. In Mach-number calculations, the effective cross section of the nozzle should be reduced by this M value over the contour. Obviously, this estimate for a flat plate allows one to judge only the order of magnitude of δ^* at the nozzle-exit cross section. To evaluate the boundary-layer thickness, one can use the formula $\delta \simeq 0.3L\sqrt{C_F}$ [8], whence $\delta \simeq 1.2 \cdot 10^{-3} \text{ m}$ and $\simeq 0.4h$.

In more accurate calculations, one should take into account the pressure gradient and the spillage effect. The estimates obtained are overrated, because the pressure gradient and the spillage effect in the supersonic nozzle decrease the thicknesses in question. It is clear, however, that the boundary layer in the nozzle can affect the supersonic-jet characteristics and hamper the use of longer nozzles.

The jet photographs presented in Figs. 2 and 3 make it possible to estimate qualitatively the thickness of the boundary layer leaving the nozzle. The light regions of the jet are characterized by density gradients in the direction perpendicular to the beam direction and can be identified with the boundary-layers leaving the nozzle, while the central dark region is associated with the jet core. Analysis of these photographs allows us to draw the conclusion that the boundary layers do not yet merge in the design exhaust of air and helium jets, and the boundary-layer thickness can be roughly estimated as $\delta = (0.3-0.4)h$.

For a more accurate estimate of the boundary-layer thickness, the velocity distribution at the nozzle exit was experimentally measured by a total-thrust probe with outside $D = 0.35 \cdot 10^{-3} \text{ m}$ and inside $d = 0.10 \cdot 10^{-3} \text{ m}$ diameters of the detection section. This probe was moved by means of a microscrew, and its location in the jet was determined from the scale of this microscrew with an accuracy of $10 \cdot 10^{-6} \text{ m}$. From the measurement data, the boundary-layer thickness was $\delta = (0.3-0.4)h$, which coincides with the presented

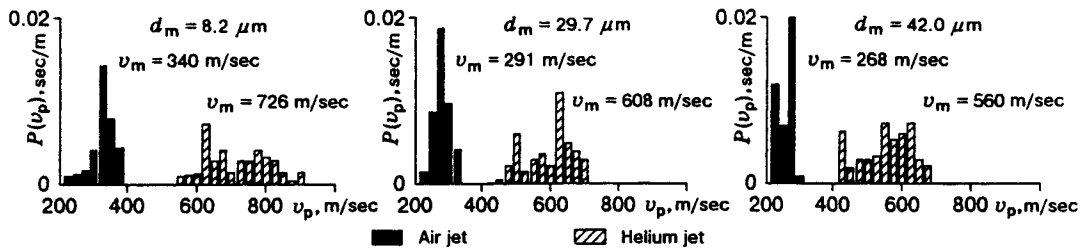


Fig. 6

above estimate obtained by optical methods (Figs. 2 and 3).

One can see that the boundary layers in the nozzle do not yet merge at the typical parameters of the nozzle ($L = 0.1$ m, $h = 3 \cdot 10^{-3}$ m, and $M = 2.0-3.0$), and the flow regime in the jet core may be treated as the design regime. This enables us to use a numerical calculation to estimate the particles velocity in the jet core during powder deposition.

4. Particle-Velocity Measurements and Comparison with Calculations. One of the most important problems was studying the influence of the particle velocity on their interaction with the substrate. For this end, it is first of all necessary to ensure the possibility of controlled variation in the particle velocity over a wide range and to develop a technique for its measurement at the nozzle exit.

The particle velocity was measured by an LDA with a direct spectral method for registration of the Doppler frequency shift (see Fig. 1). A detailed description of the method and its methodical features can be found in [9, 10]. The LDA scheme included a single-frequency helium-neon laser 15 of LG-159 type, a dividing transparent plate 16, a rotational 100% mirror 17, a polarizer for controlling the reference-beam intensity 18, focusing lenses 19 and 20, an aperture diaphragm of the optical detection system 21, a collecting lens 22, an adjusting lens 23, a multibeam confocal interferometer with a photomultiplier at the exit 24, and an oscilloscope 25. Laser-Doppler anemometers with direct spectral analysis are most effective for investigation of high-speed flows ($v_p \geq 10^2$ m/sec). Figure 5a shows a typical oscillogram obtained for the velocity of the ASD-1 particles, which was measured by the LDA method.

Another method used to measure the particles velocity in the jet at the nozzle exit is the tracking method (see Fig. 1). The main members of the setup are a ruby laser 26 operating in a free-generation regime, a telescopic system 27 and 28, an optical system forming the laser "knife" 29, a rotational 100% mirror 30, and a photodetector 13 ensuring a continuous photorecording of the moving particles. The image of the particles from the peripheral regions of the jet was cut off by a shield, and, thus, only the velocity of the particles that move in the jet core was measured. Using a fixed photodetector, it is possible to obtain the particle trajectories in the jet and also the trajectories of the incident and reflected particles. The method ensured the correct velocity measurements for particles with $d_p = (5-50) \cdot 10^{-6}$ m within the range of 200-1200 m/sec. The advantages of the method are its simplicity and its superiority to other methods of velocimetry:

- the possibility of performing measurements at very low particle concentrations when their effect on the carrying-gas parameters is ruled out altogether;
- processing of one photorecord yields simultaneously the data on the particle velocity at various distances from the nozzle exit;
- it is rather simple to obtain not only the value of the mean particle velocity, but also their velocity distribution, which is due to the particle-size distribution.

An accuracy analysis of the particle velocity found by the given method shows that the nondimensional measurement error $\Delta v_p/v_p = \Delta m/m + 2\Delta\alpha/\sin 2\alpha$ (m and Δm are the data and the accuracy of the anemometer scale of the photo recorder, respectively, and $\Delta\alpha$ is the accuracy of determination of the inclination angle of the trajectory on the film) is caused by the instrumentation accuracy and by the angular spread of the particles in the jet. Choosing the rotation velocity of the polyhedron to be photorecorded such that $\alpha = 45^\circ$ and employing appropriate detectors, one can use the method for measuring the particle velocity

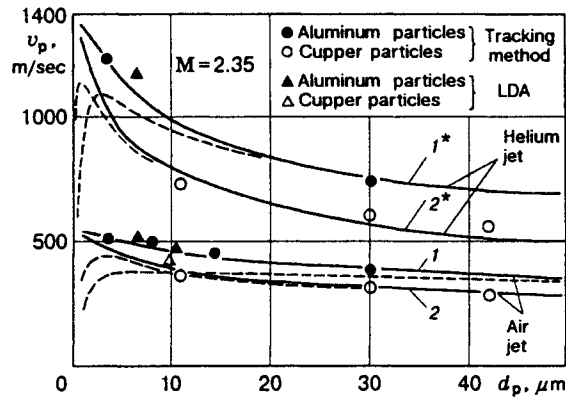


Fig. 7

with an accuracy of 10%.

We performed experiments on determination of the velocity of the particles accelerated by air and helium jets. For coatings, we utilized the scattered-in-fractions aluminum and copper particles and a large number of other powders. The necessary condition for using the tracking method is the absence of the angular spread of the particles moving in the jet core. To verify this, the particles leaving the nozzle were photographed by the laser-“knife” method. A ruby laser used in a free-generation regime as a light source allowed us to register the tracks of these particles. Analysis of the photographs showed that the particles in the jet core move parallel to its axis without the angular spread.

Figure 5b illustrates a photorecord of the moving aluminum particles of fraction $d_p = (40-50) \cdot 10^{-6}$ m. Processing of such photo records with a microscope by measuring the trajectory inclination angle of a moving particle to the film axis enabled us to find the velocity of each individual particle at various distances from the nozzle exit which was varied within the range of $0-30 \cdot 10^{-3}$ m. The measurements showed that the particle velocity was nearly constant in the jet-core region considered. On the basis of these measurements, we considered the particle velocity-distribution functions which are due to the particle-size distribution. The mean particle velocity $v_m = \Sigma v_p^i / N$ and the distribution variance $\sigma_v = \Sigma (v_p^i - v_m)^2 / (N - 1)$ were found by processing the measurement results (v_p^i is the velocity of an individual particle).

The velocity-distribution functions were measured for the dispersed fractions of aluminum and copper particles when the particles were accelerated by air or helium under design flow conditions in nozzles with $L = 0.07, 0.1, \text{ and } 0.13$ m. The results shown in Fig. 6 illustrate clearly the effect of the particle sizes and of the test gas composition on the particle velocity. In addition, the velocity-distribution functions P of various copper fractions accelerated by the air and helium jets are plotted in this figure.

The results of experimental determination of the velocity of different particles at the nozzle exit were compared with numerical results and are presented in Fig. 7 as curves of the particle velocity versus the particle size. The solid curves refer to the results of numerical calculations of the particle velocity at the nozzle exit which were accelerated by the air jet (curves 1 and 2) and by the helium jet (curves 1* and 2*). This figure also shows the experimentally determined velocity of these particles obtained under the conditions adopted in calculations. Good agreement of the numerical and experimental results allows us to consider these data reliable and to use the calculations for further estimation of the particle velocity during deposition.

Figure 7 also shows the calculated velocities of the aluminum and copper particles near the substrate surface (dashed curves). The light particles lose markedly their velocity in the gas-stagnation region immediately upstream of the substrate. The copper particles are more inertial, they have a lower velocity at the nozzle exit, but are less decelerated behind the shock wave. As a result, both copper and aluminum particles with sizes of $(5-20) \cdot 10^{-6}$ m strike the substrate at an approximately equal velocity (~ 400 m/sec) when they are accelerated by the air jet. In the helium jet, the effect of the particle inertia on their final velocity is even more pronounced. The results show that to obtain a sufficiently high particle velocity at the

substrate, one should not only choose the optimum length of the nozzle but also weaken the unfavorable decelerating effect of the compressed gas immediately upstream of the substrate.

Thus, the results presented demonstrate the efficiency of application of plane supersonic jets for deposition, since such jets ensure a maximum impact velocity of particles against a substrate owing to decrease in the compressed-gas thickness layer ahead of a target and, hence, its minimum decelerating effect on the particles. The technique for controlling and determining the particle velocity within the range of 200–1200 m/sec, which was worked out on the basis of experimental data, allowed us to change over to experimental investigations of the basic features of the formation of coatings from solid-state particles distinguished by material, velocity, size, etc.

REFERENCES

1. Yu. S. Borisov, Yu. A. Kharlamov, S. L. Sidorenko, and E. N. Ardatovskaya, *Gas-Thermal Coatings of Powder Materials: Handbook* [in Russian], Naukova Dumka, Kiev (1987).
2. V. V. Kudinov and V. M. Ivanov, *Plasma-Deposited High-Melting Coatings* [in Russian]. Mashinostroenie, Moscow (1981).
3. B. S. Mitin (ed.), *Powder Metallurgy and Deposited Coatings* [in Russian], Metallurgiya, Moscow (1987).
4. A. P. Alkhimov and A. N. Papyrin, Russian Patent No. 1618782, "Method of obtaining aluminum coatings," in: *Otkr. Izobr.*, No. 1 (1991).
5. V. G. Dulov (ed.), *Supersonic Gas Jets* [in Russian], Nauka, Novosibirsk (1983).
6. H. Schlichting, *Boundary Layer Theory*, McGraw-Hill, New York (1968).
7. Yu. V. Lapin, *Turbulent Boundary Layer in Supersonic Gas Flows* [in Russian], Nauka, Moscow (1983).
8. L. D. Landau and M. I. Lifshits, *Hydrodynamics* [in Russian], Nauka, Moscow (1988).
9. A. P. Alkhimov, A. N. Papyrin, R. I. Soloukhin, et al., "A laser-Doppler anemometer for investigation of gas-dynamic flows," *Fiz. Goreniya Vzryva*, No. 4, 585–596 (1973).
10. A. P. Alkhimov, A. N. Papyrin, A. L. Predein, and R. I. Soloukhin, "An experimental study of the effect of particle-velocity delay in a supersonic gas flow," *Prikl. Mekh. Tekh. Fiz.*, No. 4, 80–87 (1977).